

Cosmological Constraints on Decoupled Dark Photons and Dark Higgs

Joshua Berger^a, Karsten Jedamzik^b and Devin G. E. Walker^c

^a*Department of Physics, University of Wisconsin-Madison, Madison, WI 53706, USA*

^b*Laboratoire Univers et Particules de Montpellier, UMR5299-CNRS,
Université Montpellier II, 34095 Montpellier, France and*

^c*Department of Physics, University of Washington, Seattle, WA 98195, USA*

Any neutral boson such as a dark photon or dark Higgs that is part of a non-standard sector of particles can mix with its standard model counterpart. When very weakly mixed with the Standard Model, these particles are produced in the early Universe via the freeze-in mechanism and subsequently decay back to standard model particles. In this work, we place constraints on such mediator decays by considering bounds from Big Bang nucleosynthesis and the cosmic microwave background radiation. We find both nucleosynthesis and CMB can constrain dark photons with a kinetic mixing parameter between $\log \epsilon \sim -10$ to -17 for masses between 1 MeV and 100 GeV. Similarly, the dark Higgs mixing angle ϵ with the Standard Model Higgs is constrained between $\log \epsilon \sim -6$ to -15 . Dramatic improvement on the bounds from CMB spectral distortions can be achieved with proposed experiments such as PIXIE.

Contents

I. Introduction	1
II. Mediator Models	2
A. Dark Higgs Mixing and Couplings	2
B. Dark Photon Mixing and Couplings	3
III. Freeze-In Production of Mediators	4
A. Dark Photon Freeze-In Production	5
B. Dark Higgs Freeze-In Production	5
IV. Mediator Decays	6
A. Dark Photon Decays	6
B. Dark Higgs Decays	7
V. Nucleosynthesis Constraints	8
A. BBN Constraints on Dark Photons	10
B. BBN Constraints on Dark Higgses	12
VI. Cosmic Microwave Background Constraints	13
A. CMB Constraints on Dark Photons	15
B. CMB Constraints on Dark Higgs	15
VII. Conclusions	15
References	17

I. INTRODUCTION

Cosmological evidence indicates that the majority of matter in the universe is non-baryonic dark matter. Given its cosmological importance, there is little reason to believe that dark matter is part of some simple, inert sector. The interactions of the dark sector could be as complex as those of our own visible sector. Bosons that mediate dark matter self-interactions could also form a portal by which the SM can interact weakly with dark matter. In

such a scenario, a neutral gauge/scalar boson mediator mixes with the SM counterpart photon- Z /Higgs systems. The neutral gauge boson particles are referred to as dark photons [1–5] (even though they also mix in part with the Z boson), while the neutral scalar boson particles are referred to as dark Higgs [6–21]. These interactions could well dominate the interaction between the dark and visible sectors as they are among the only possible renormalizable interactions of a dark sector with the SM.

As such, portal interactions have been studied extensively [22–42]. Much of the focus has been on the region of relatively large mixing, wherein the mediator itself is in thermal equilibrium with the SM bath in the early universe before rapidly decaying when $H < \Gamma$. Constraints on mediators in such scenarios arise from a combination of laboratory experiments such as beam dumps and lepton colliders, as well as astrophysical constraints from supernovae for lighter mediators [43–69]. Their direct effect on cosmology is negligible since they decay well before the epochs we can study observationally, i.e. Big Bang Nucleosynthesis (BBN) and recombination. On the other hand, for smaller mixing angles, the mediator can be sufficiently long lived to decay during or after one of these events, opening the door for a new set of constraints that restrict mediator parameter space at small mixing angles.

In order for the mediators to have a significant effect, they must be produced in non-negligible quantities. This is however the case, since even under the pessimistic assumption that no mediators were present in the very early universe, such as the period just after inflaton decay, a sufficient abundance will be “frozen-in” by mixing with the SM bosons so as to constrain much of the parameter space. This process of mediator freeze-in could also lead to the generation of a significant abundance of dark matter, though we leave the study of such an effect to future work.

In this work we characterize the effect of the mediator decays on nucleosynthesis and the CMB. We show, even in the limit where the mediators have a small coupling with the Standard Model, large regions of parameter space are excluded. We note, however, that our constraints do evaporate in case these dark mediators decay into lighter stable dark sector particles before decaying into standard model particles. Constraints on weakly mixed dark photons with Stueckelberg masses were published previously in Ref. [70]. Our analysis significantly improves on their study by correcting some errors and negligence in their BBN treatment.

The remainder of this paper is structured as follows. In Section II, we review the dark photon and dark Higgs models. Subsequently, we study the production and decay of mediators in Sections III and IV. We then present constraints on both models in Sections V and VI. Finally, we conclude in Section VII.

II. MEDIATOR MODELS

We consider a generic scenario where the Standard Model (SM) gauge group is extended by an additional $U(1)_D$ which we refer to as dark hypercharge. A dark Higgs is introduced to spontaneously break $U(1)_D$ and give mass to the corresponding dark photon.

A. Dark Higgs Mixing and Couplings

In the minimal model, an additional scalar boson Φ charged under a new $U(1)_D$ gauge group is introduced. The scalar boson gets a vacuum expectation value that breaks $U(1)_D$, giving mass to the dark Higgs. We parametrize the Higgs fields as

$$H = \frac{1}{\sqrt{2}} \begin{pmatrix} 0 \\ v + h \end{pmatrix} \quad \Phi = \frac{1}{\sqrt{2}}(u + \rho), \quad (\text{II.1})$$

neglecting the Goldstone modes which get eaten. While we shortly consider potential kinetic mixing between the $U(1)_D$ and $U(1)_Y$ gauge bosons, we first consider mixing between ρ and the SM Higgs field H . The most general scalar potential after symmetry breaking can be written as

$$V = \lambda_1 \left(H^\dagger H - \frac{v^2}{2} \right)^2 + \lambda_2 \left(\Phi^\dagger \Phi - \frac{u^2}{2} \right)^2 + \lambda_3 \left(H^\dagger H - \frac{v^2}{2} \right) \left(\Phi^\dagger \Phi - \frac{u^2}{2} \right). \quad (\text{II.2})$$

The λ_3 coupling mixes the visible and dark Higgs sectors. The physical Higgs masses are

$$m_h^2 = 2\lambda_1 v^2 \left(1 - \frac{\lambda_3^2}{4\lambda_1\lambda_2} + \dots\right) \quad m_\rho^2 = 2\lambda_2 u^2 \left(1 + \frac{\lambda_3^2}{4\lambda_2^2} \frac{v^2}{u^2} + \dots\right) \quad (\text{II.3})$$

where m_h is the SM Higgs mass and is fixed to 125 GeV [71]. m_ρ is the dark Higgs mass. The Higgses will mix as

$$\begin{pmatrix} h' \\ \rho' \end{pmatrix} = \begin{pmatrix} \cos \epsilon & \sin \epsilon \\ -\sin \epsilon & \cos \epsilon \end{pmatrix} \begin{pmatrix} h \\ \rho \end{pmatrix}, \quad (\text{II.4})$$

where the primes denote the mass eigenstates. For brevity going forward, we refer to both the mass eigenstates without primes. The mixing angle is given by

$$\tan 2\epsilon = \frac{\lambda_3 uv}{\lambda_1 v^2 - \lambda_2 u^2} \quad (\text{II.5})$$

In the limit where $\lambda_3 uv \ll \lambda_1 v^2, \lambda_2 u^2$, which is the limit considered in this work, the mixing angle can be written as

$$\tan 2\epsilon = \frac{2\lambda_3 uv}{m_h^2 - m_\rho^2}. \quad (\text{II.6})$$

Given equation (II.4), the SM fermion coupling to the mass eigenstate dark Higgs is simply a rescaling of the SM coupling,

$$y_{\bar{f}f\rho} = -\frac{ig m_f}{2 m_W} \sin \epsilon. \quad (\text{II.7})$$

There are enough free parameters to treat the dark Higgs mass and mixing parameters as independent parameters and we do so in this work. The corresponding coupling between the SM Higgs and the SM fermions is proportional to $\cos \epsilon$. Because we are interested in the regime of parameter space where $\sin \epsilon$ is very small, constraints on SM Higgs couplings from the LHC are not applicable [72, 73].

Note that there are actually 3 new parameters in this model, which we can take to be either λ_2 , λ_3 and u , or more conveniently m_ρ , ϵ , and λ_3 . While most of the dark Higgs couplings to the SM depends only on ϵ and kinematics depends only on m_ρ , the $\rho^2 h^2$ coupling depends directly on λ_3 . We can consistently take the limit $\lambda_3 \rightarrow 0$, holding ϵ fixed by simultaneously taking $u \rightarrow \infty$. In this work, we adopt such a limit, which is the most conservative option: deviation from this limit would enhance dark Higgs production, while keeping the lifetime fixed. The extra dark Higgs abundance can only enhance constraints.

B. Dark Photon Mixing and Couplings

The dark Higgs also generates a mass for the dark photon. In this section, we focus on the properties of this massive gauge boson. For concreteness, we take $Q_D = 2$ for the dark Higgs, though this choice is arbitrary up to a rescaling of the dark gauge coupling. The gauge sector lagrangian is

$$\mathcal{L}_{\text{gauge}} = -\frac{1}{4} \hat{B}_{\mu\nu} \hat{B}^{\mu\nu} - \frac{1}{4} \hat{F}'_{\mu\nu} \hat{F}'^{\mu\nu} - \frac{\epsilon}{2} \hat{B}_{\mu\nu} \hat{F}'^{\mu\nu}, \quad (\text{II.8})$$

where ϵ is the coupling of the kinetic term and links the dark and visible $U(1)_Y$ gauge sectors. Because of this coupling, any SM particle with non-zero hypercharge will then acquire a dark charge. Because the $U(1)_D$ gauge boson mixes with hypercharge, the dark photon will have chiral couplings to the SM fermions. The axial component, however, is suppressed in the limit that $m_{\gamma'} \ll m_Z$, as we see explicitly below. Without loss of generality, we parametrize this coupling as $\epsilon = \sin \delta$ [5]. The kinetic terms can be diagonalized by defining new fields B_μ and A'_μ such that

$$\begin{pmatrix} \hat{B}_\mu \\ \hat{A}'_\mu \end{pmatrix} = \begin{pmatrix} 1 & -\tan \delta \\ 0 & \sec \delta \end{pmatrix} \begin{pmatrix} B_\mu \\ A'_\mu \end{pmatrix} \quad (\text{II.9})$$

where the hatted fields are the fields before diagonalizing the kinetic mixing. After this rotation, equation (II.8) is diagonalized. However, a mixing is induced in the mass matrix for the gauge bosons. After doing the standard Weinberg angle diagonalization, we have

$$|D_\mu H|^2 + |D_\mu \phi|^2 \supset \frac{1}{2} m_Z^2 Z^2 + \frac{1}{2} m_{\gamma'}^2 A'^2 + \delta m^2 Z A' \quad (\text{II.10})$$

where

$$m_Z^2 = \frac{1}{4} v^2 (g_1^2 + g_2^2) \quad (\text{II.11})$$

$$m_{\gamma'}^2 = \frac{1}{4} v^2 g_1^2 \tan^2 \delta + 4 u^2 g'^2 \sec^2 \delta \quad (\text{II.12})$$

$$\delta m^2 = -\frac{1}{4} v^2 g_1 \sqrt{g_1^2 + g_2^2} \tan \delta. \quad (\text{II.13})$$

We can diagonalize the mass term by introducing a mass mixing angle ξ defined by

$$\tan 2\xi = \left(\frac{2 m_Z^2}{m_Z^2 - m_{\gamma'}^2} \right) \sin \theta_W \tan \delta. \quad (\text{II.14})$$

In the limit of small kinetic mixing, the mass eigenstates are approximately the charge eigenstate mass terms given in equations (II.11) and (II.12). The coupling between the SM fermions, f , and the dark photon is

$$g_{ff\gamma'} = -i \gamma^\mu (g'_V + g'_A \gamma_5). \quad (\text{II.15})$$

where

$$g'_V = -e\epsilon \left(Q \frac{c_W^2 m_Z^2 - m_{\gamma'}^2}{c_W(m_Z^2 - m_{\gamma'}^2)} - T_3 \frac{m_{\gamma'}^2}{2c_W(m_Z^2 - m_{\gamma'}^2)} \right) \quad g'_A = e\epsilon T_3 \frac{m_{\gamma'}^2}{2c_W(m_Z^2 - m_{\gamma'}^2)} \quad (\text{II.16})$$

Here c_W is the cosine of the Weinberg angle with $c_W^2 \approx 0.775$. Thus, for the SM fermion, f , the only unknown parameter is the kinetic mixing parameterization. In the limit $m_{\gamma'} \ll m_Z$, this is proportional to the photon couplings to f :

$$g'_V \approx -c_W e Q \epsilon \quad g'_A \approx 0 \quad (\text{II.17})$$

As in the Higgs case, there are enough free parameters to treat the dark photon mass and mixing as independent parameters.

III. FREEZE-IN PRODUCTION OF MEDIATORS

As emphasized above, we are considering scenarios in which the mixing between the mediator and the SM is very small. Thus, the rate at which the mediator interacts with the SM is much less than the Hubble rate at all times over the vast majority of parameter space¹. Even if the mediator never equilibrates with the SM, it can be produced non-thermally and have observable effects on cosmological evolution. In the limit of such small mixing, the mediators can be produced via two mechanisms: decay of heavy, non-standard particles and freeze-in. We adopt a conservative approach and assume only a negligible amount of mediator particles are produced by early decays of non-standard particles, including any inflatons. The abundance is then entirely determined by freeze-in production mediated by SM particles [74]. In this section, we determine the freeze-in abundance of both dark photons and dark Higgs.

Provided the coupling of the mediator to light particles is similar to the coupling of the mediator to heavy particles, then mediator production will be dominated by inverse decay processes. Processes with a higher number of initial states are phase space suppressed. This criterion is in fact satisfied in the case of the dark photon, where the coupling between all standard model particles and the mediator are comparable. In the case of the dark Higgs, however, the coupling to particles is proportional to their mass. We find that the additional phase space suppression of $2 \rightarrow 2$ processes is more than overcome by the larger coupling to heavy particles and production is dominated by top quark annihilation and inelastic scattering.

¹ For some portions of the dark Higgs parameter space considered in this work, the mediator production becomes large and equilibrium is reached. However, we do not attempt to further study such portions of parameter space.

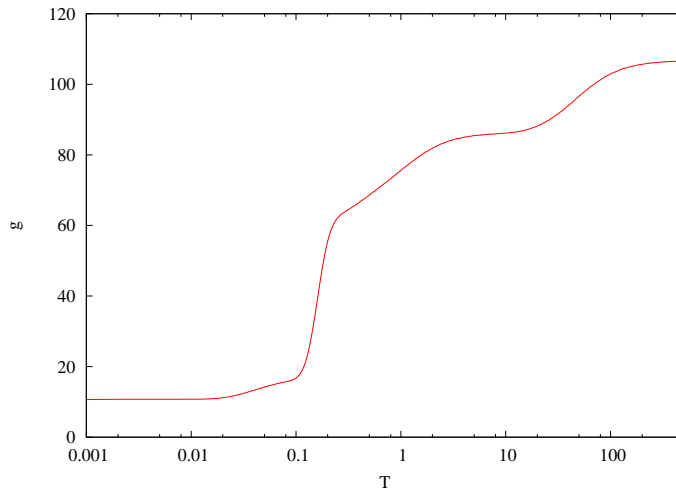


FIG. 1: The relativistic degrees of freedom $g(T)$ as a function of temperature T in GeV.

A. Dark Photon Freeze-In Production

The dominant production of dark photons comes from inverse decay of charged species. We assume that $m_{\gamma'} < 2m_W$, so that the decays are to charged fermions: quarks and leptons. The decay rate of the dark photon to species ψ_i can be written as

$$\Gamma_i \equiv \Gamma(\gamma' \rightarrow \psi_i \bar{\psi}_i) = \epsilon^2 \frac{N_c c_W^2 Q_i^2 \alpha}{3} m_{\gamma'} \left(1 - \frac{4m_i^2}{m_{\gamma'}^2}\right)^{1/2}, \quad (\text{III.1})$$

where N_c is the number of colors for species i . The freeze-in production of the dark photon is most easily computed by the principle of detailed balance, i.e. the thermal rate for inverse decay production equals that of the decay rate of the dark photon with a putative equilibrium distribution

$$\frac{dn_{\gamma'}}{dt} = \int_0^\infty \frac{d^3 p_{\gamma'}}{(2\pi)^3} \frac{f_{\gamma'}^{eq} \Gamma_{\gamma'}}{E_{\gamma'}/m_{\gamma'}}, \quad (\text{III.2})$$

where

$$f_{\gamma'}^{eq} = \frac{g_{\gamma'}}{e^{E_{\gamma'}/T} - 1} \quad (\text{III.3})$$

is the dark photon equilibrium distribution with $g_{\gamma'} = 3$ the dark photon number of degrees of freedom and where $\Gamma_{\gamma'} = \sum_i \Gamma_i$ is the total width of the dark photon.

This expression may be used to compute the asymptotic dark-photon-to-entropy ratio $Y_{\gamma'} = n_{\gamma'}/s$, produced by inverse decay of fermions in the early Universe at temperatures $T \gtrsim m_{\gamma'}$

$$Y(t \rightarrow \infty) \approx \frac{g_{\gamma'}}{g(m_{\gamma'})} \frac{90}{\pi^4} \frac{\Gamma_{\gamma'}}{H(m_{\gamma'})}, \quad (\text{III.4})$$

where $H(T)$ is the Hubble scale at temperature T . The largest contribution to the dark photon abundance comes from temperatures of order the dark photon mass. The dark photon abundance Y increases as $1/T^3$ before reaching a maximum at $T \sim m_{\gamma'}$. Eq. (III.4) is only correct up to a factor of order unity. This is mostly due to an assumed constancy of the relativistic degrees of freedom during the final phases of freeze-in. As may be seen from Fig. 1 the relativistic degrees of freedom change drastically particularly during the QCD epoch. Results given below include are exact as Eq. (III.2) is numerically integrated for the analysis.

B. Dark Higgs Freeze-In Production

The determination of the dark Higgs abundance involves the $2 \rightarrow 2$ processes of top quark annihilation and inelastic scattering as shown in Figure 2. These processes freeze-in at temperatures $T \lesssim m_t$. Assuming that $m_\rho \ll m_t$,

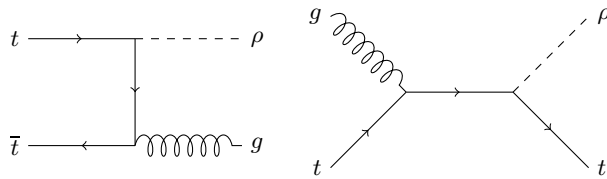


FIG. 2: Dominant diagrams for the production of dark Higgs bosons. Both processes have an additional u -channel process that is not illustrated.

the dark Higgs mass can be neglected. These processes only turn on after the electroweak phase transition, but nevertheless dominate production. The total cross-sections for these processes are then given by

$$\sigma(t\bar{t} \rightarrow \rho g) = \frac{2\pi\epsilon^2\alpha_s\alpha m_t^2[\sqrt{s(s-4m_t^2)}(s^2 - 12m_t^2s + 8m_t^4) - 2(s^3 - 7s^2m_t^2 + 8m_t^4s - 16m_t^6)\arctan\sqrt{1-4m_t^2/s}]}{9m_W^2(m_t^2 - s)s^2(s - 4m_t^2)s_W^2} \quad (\text{III.5})$$

and

$$\sigma(tg \rightarrow t\rho) = \frac{\pi\epsilon^2\alpha_s\alpha m_t^2[2s^2(3m_t^2 + s)^2 \log(m_t^2/s) - (s - m_t^2)(m_t^2 + 3s)(m_t^4 - 8m_t^2s - s^2)]}{24m_W^2s^2s_W^2(s - m_t^2)^3} \quad (\text{III.6})$$

respectively. Thermally averaging² and solving the Boltzmann equation numerically, we find

$$Y(t \rightarrow \infty) \approx (0.27 + 0.42) \frac{\epsilon^2\alpha\alpha_s m_\rho^5 m_t^2}{8\pi^3 H(m_\rho) s(m_\rho) m_W^2 s_W^2}, \quad (\text{III.7})$$

where the first number denotes the contribution from annihilation and the second denotes the contribution from inelastic scattering of t and \bar{t} . Note that this result depends only on the mixing angle ϵ in the limit that $m_\rho \ll m_t$. Numerically, we find

$$Y(t \rightarrow \infty) \approx 1.6 \times 10^{12} \times \epsilon^2 \quad (\text{III.8})$$

IV. MEDIATOR DECAYS

Once the universe has cooled such that $\Gamma \sim H$, the mediator will decay rapidly. The consequences of this decay depend both on when the decay occurs and on what the dominant decay products are. The Hubble rate during the period of BBN and during recombination are well-known within standard cosmology, so given a determination of the decay rate, we can determine the parameter space that can potentially be covered by the analysis in this work. We now present our determination of both the total decay width and the branching fractions of the mediators.

A. Dark Photon Decays

The dark photon decays to any charged particles with $m < m_{\gamma'}/2$. Decays to color neutral particles, which is to say leptons in the part of parameter space considered here, are straightforwardly determined using (III.1). The hadronic width and branching fractions are somewhat more involved. Since the dark photon couples to the electromagnetic current, hadronic decays can be related to the hadron-to-muon cross-section ratio in e^+e^- interactions via

$$\Gamma(\gamma' \rightarrow \text{hadrons}) = R(E_{\text{CM}} = m_{\gamma'})\Gamma(\gamma' \rightarrow \mu^+\mu^-). \quad (\text{IV.1})$$

² In doing so, we neglect backreaction terms for stimulated emission and fermi blocking. Such terms are expected to have at most an $\mathcal{O}(1)$ effect in the relevant regime.

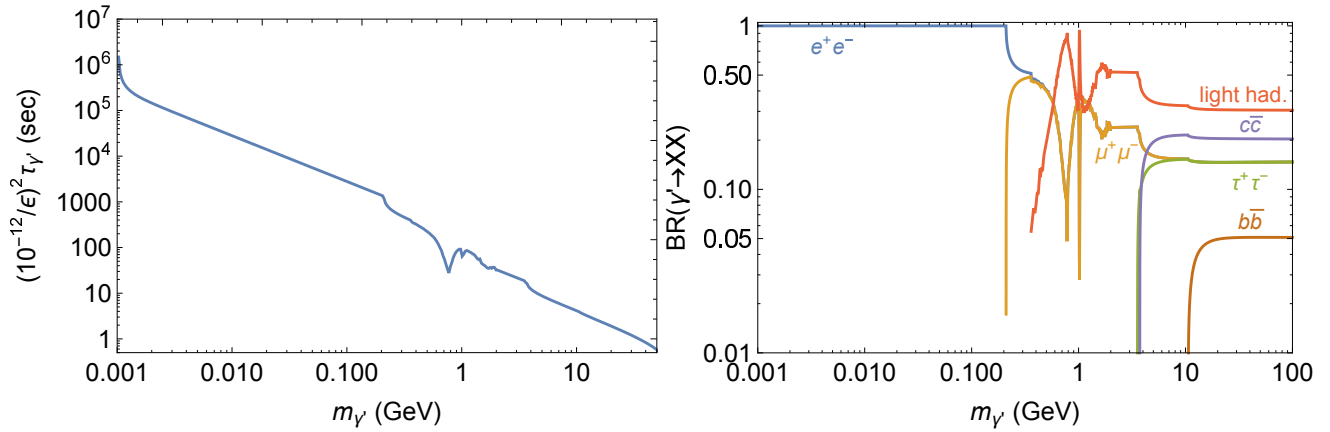


FIG. 3: Lifetime and branching fraction of a dark photon. The lifetime becomes short when resonant hadronic decay occurs, as for example at ~ 750 MeV, the approximate mass of the ω -resonance.

For $m_{\gamma'} \gtrsim 2$ GeV, the ratio R can be accurately determined in perturbative QCD via

$$R(m_{\gamma'}) = 3 \sum_f Q_f^2 \frac{(m_{\gamma'}^2 + 2m_f^2) \sqrt{m_{\gamma'}^2 - 4m_f^2}}{(m_{\gamma'}^2 + 2m_\mu^2) \sqrt{m_{\gamma'}^2 - 4m_\mu^2}} \left(1 + \frac{\alpha_s}{\pi} + \mathcal{O}(\alpha_s^2) \right). \quad (\text{IV.2})$$

The exclusive number of each type of quasi-stable hadron has been determined using PYTHIA 6 [75] to simulate a parton shower and hadronization in e^+e^- collisions at $E_{\text{CM}} = m_{\gamma'}$.

For $m_{\gamma'} \lesssim 2$ GeV, we use data-driven methods to determine both R and the fragmentation into exclusive final states. The ratio has been determined by summing the various exclusive final states in several experiments at low energies and a combination of these has been presented by the Particle Data Group [76, 77]. We then determine the fragmentation into quasi-stable hadrons using the measured branching fractions of the few resonances that contribute to R at low energies.

The resulting total decay width and branching fractions are shown in Figure 3.

B. Dark Higgs Decays

The dark Higgs decays with couplings that are proportional to those of the SM Higgs. For $m_\rho \gtrsim 2$ GeV, we once more turn to a perturbative determination of the dark Higgs decay width and inclusive branching fractions. Unlike in the dark photon case, decays to pairs of gauge bosons (namely gluons and photons) are allowed and can be significant in certain parts of parameter space. The partial widths to fermions are determined at leading order by

$$\Gamma(\rho \rightarrow f\bar{f}) = \sin^2 \epsilon \frac{G_f m_f^2}{4\sqrt{2}\pi} m_\rho \left(1 - \frac{4m_f^2}{m_\rho^2} \right)^{3/2} \quad (\text{IV.3})$$

For decays to quarks, an NLO correction factor of [78]

$$1 + 5.67 \frac{\alpha_s}{\pi} + \mathcal{O}(\alpha_s^2) \quad (\text{IV.4})$$

is applied. The decays to gluons and photons (including a NLO correction for the gluon case [79]) are given by

$$\Gamma(\rho \rightarrow gg) = \sin^2 \epsilon \frac{G_f \alpha_s^2 m_\rho^3}{64\sqrt{2}\pi^3} \left| \sum_q F_{1/2}(\tau_q) \right|^2 \left(1 + \frac{215}{12} \frac{\alpha_s}{\pi} + \mathcal{O}(\alpha_s^2) \right) \quad (\text{IV.5})$$

and

$$\Gamma(\rho \rightarrow \gamma\gamma) = \sin^2 \epsilon \frac{G_f \alpha^2 m_\rho^3}{128\sqrt{2}\pi^3} \left| \sum_f N_{c,f} Q_f^2 F_{1/2}(\tau_f) + F_1(\tau_W) \right|^2 \left(1 + \frac{215}{12} \frac{\alpha_s}{\pi} + \mathcal{O}(\alpha_s^2) \right) \quad (\text{IV.6})$$

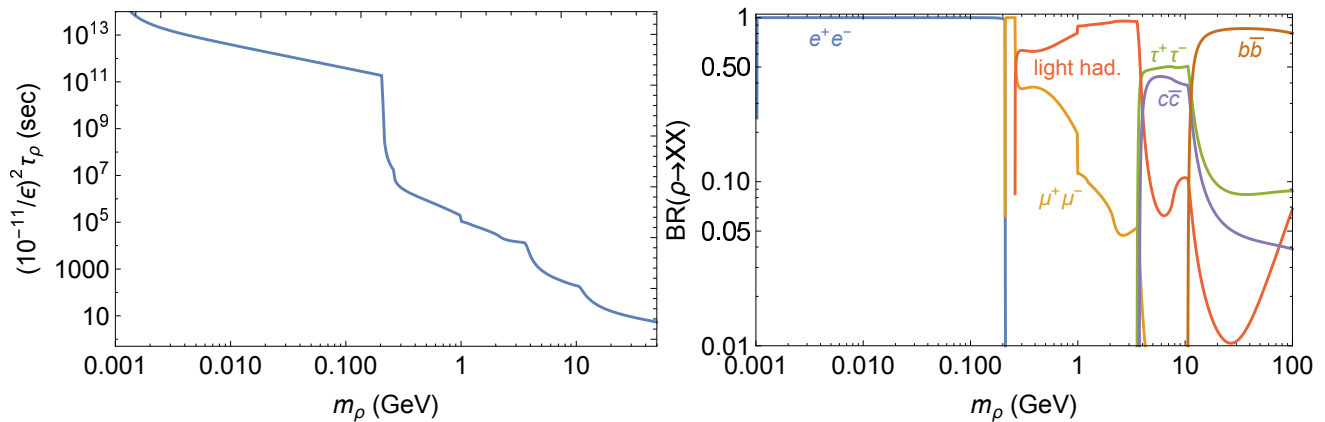


FIG. 4: Lifetime and branching fraction of a dark Higgs. Note that the branching ratio to two photons is exceedingly small and therefore not seen in the figure.

respectively, with $\tau_i \equiv 4m_i^2/m_\rho^2$. F_i are well-known loop functions, given explicitly in [80] for example. The exclusive fragmentation into quasi-stable hadrons is once again determined using PYTHIA 6 [75]. In this case, we simulate $e^+e^- \rightarrow h$ production at $E_{\text{CM}} = m_\rho$.

For $m_\rho \lesssim 2$ GeV, there is no purely data-driven method for determining the decay width and branching fractions as the SM Higgs is far too heavy and weakly coupled to be seen in low-energy e^+e^- collisions. There is some degree of controversy surrounding such decays, with several methods presenting vastly different results. In this work, for masses below 1 GeV, we use a determination based on low energy theorems, while we continue to use a perturbative calculation down to around 1 GeV, where the two methods overlap. It is worth noting that light scalar resonances can distort these results.

Low energy theorems predict decay widths of [81, 82]

$$\Gamma(\rho \rightarrow M\bar{M}) = \frac{1}{81} \frac{m_\rho^2}{m_\mu^2} \left(1 + \frac{11}{2} \frac{m_M^2}{m_\rho^2}\right)^2 \frac{(1 - 4m_M^2/m_\rho^2)^{1/2}}{(1 - 4m_\mu^2/m_\rho^2)^{3/2}} \Gamma(\rho \rightarrow \mu^+\mu^-), \quad (\text{IV.7})$$

where $M\bar{M}$ are all isospin combinations ($2 \pi^+\pi^-$, $\pi^0\pi^0$, $2 K\bar{K}$, and $2 K^+K^-$ being the relevant ones for our study— η is too heavy to contribute before we switch to a perturbative calculation). The resulting decay width and branching fractions are shown in Figure 4.

V. NUCLEOSYNTHESIS CONSTRAINTS

It is well known that quasi-stable particles with decay times $\tau \gtrsim 0.1$ seconds may significantly perturb the primordial light element nucleosynthesis occurring approximately between 1 and 1000 seconds after the birth of the universe [77]. Comparing the observationally inferred primordial abundances with the predicted ones, we are able to derive limits on the abundance and lifetimes of these putative relic particles. In the previous sections, we have derived the frozen-in abundances for dark Higgses and dark photons for a generic model. In this section, we consider the constraints on the model parameter space from Big Bang nucleosynthesis (BBN).

When the quasi-stable mediators decay, their energetic decay products can perturb BBN by either hadronic or electromagnetic interactions with the particles in the baryon-photon plasma. In particular, the injection of mesons between $\tau \sim 0.1$ -10 seconds may alter the neutron-to-proton ratio via charge exchange reactions, and thereby elevate the primordial helium mass fraction Y_p beyond its observational upper limit. The injection of energetic nucleons at $\tau > 100$ seconds produces a cascade of secondary and tertiary energetic nucleons which are capable of spalling ^4He , thereby producing neutrons, ^2H , ^3H , and ^3He . The resulting neutrons may form ^2H via non-thermal fusion of protons. Energetic ^3H and ^3He may fuse on ^4He to form ^6Li to generate an abundance orders of magnitude larger than what predicted in standard BBN. Injection of energetic electromagnetically interacting particles, on the other hand, produce a cascade on the cosmic microwave background (CMB) radiation, with the resulting gamma-rays capable of photo-disintegrating ^2H for $\tau \gtrsim 10^5$ seconds and ^4He for $\tau \gtrsim 3 \times 10^6$ seconds. Altogether, there are $\mathcal{O}(100)$ hadronic and electromagnetic interactions that are important. See [83] for additional details.

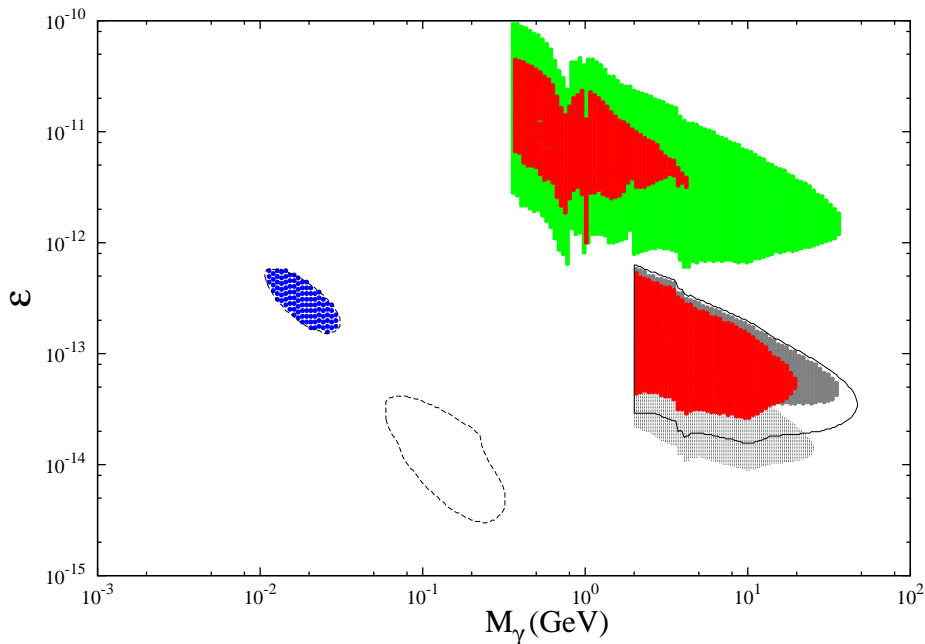


FIG. 5: Constraints on the dark photon mixing ϵ -mass $m_{\gamma'}$ parameter space from Big Bang nucleosynthesis. Colored shaded regions are ruled out. Shaded green and red areas are ruled out from ${}^4\text{He}$ and ${}^2\text{H}$ overproduction, respectively. In shaded blue areas ${}^2\text{H}$ is underproduced. In the light grey areas a substantial ${}^6\text{Li}$ abundance is produced (i.e. ${}^6\text{Li}/{}^7\text{Li} > 0.1$), whereas in the dark shaded areas the ${}^7\text{Li}$ abundance is reduced to an observationally favored ${}^7\text{Li}/\text{H} < 2.5 \times 10^{-10}$. The solid line shows how much the red area ruled out due to ${}^2\text{H}$ overproduction would increase if a more stringent, less conservative, ${}^2\text{H}/\text{H} < 3 \times 10^{-5}$ (versus 4×10^{-5} limit) would be imposed. This indicates that solutions to the cosmological ${}^7\text{Li}$ problem only exist in models which predict ${}^2\text{H}/\text{H} > 3 \times 10^{-5}$. Finally, in the region within the dotted line a mild increase of the ${}^3\text{He}/{}^2\text{H}$ ratio occurs. The ratio nevertheless does not surpass either one or the observational limit of 1.5.

In the following analysis, we adopt the following observational inferred constraints on primordial light-element abundances:

$${}^2\text{H}/\text{H} < 4 \times 10^{-5} \quad (\text{V.1})$$

from quasar absorption systems at high redshift [84–86]. In addition,

$${}^2\text{H}/\text{H} > 2 \times 10^{-5}, \quad (\text{V.2})$$

from deuterium abundances in the local interstellar medium [87]. Here it is noted that a recent determination of the primordial deuterium abundance of $2.53 \pm 0.04 \times 10^{-5}$ [86] in a number of damped Lyman- α systems would substantially increase the parameter space which is ruled out. However, we do not use these very stringent limits as it has not been established that prior determinations of ${}^2\text{H}/\text{H}$ in lower column density quasar absorption systems going to values as large as 5.3×10^{-5} [84, 85] (at two sigma) may be flawed. We feel that the recent determination could actually be biased to demonstrate concordance between the standard BBN prediction at a precisely inferred baryon density from observations of the cosmic microwave background radiation (hereafter, CMBR) and observations. Though this concordance generally exists, the presented new analysis does not provide significant observational improvements to warrant such a large reduction of observational error bars. It has been shown that ${}^3\text{He}/{}^2\text{H}$ is an important diagnostic [88] and we adopt

$${}^3\text{He}/{}^2\text{H} < 1.5, \quad (\text{V.3})$$

from the deuterium and ${}^3\text{He}$ abundance in the presolar nebula [89]. The upper limit on the helium mass fraction Y_p is taken to be

$$Y_p < 0.26, \quad (\text{V.4})$$

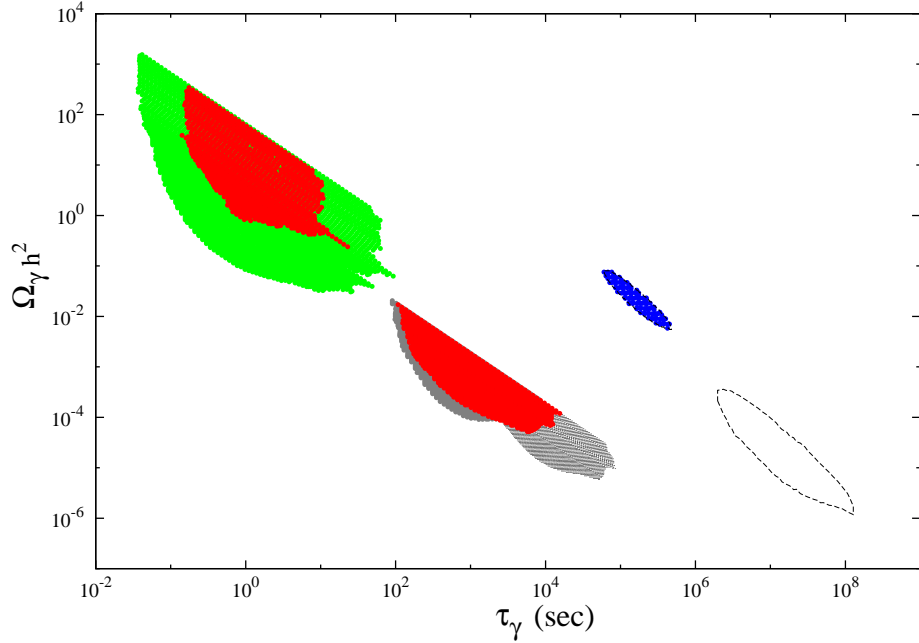


FIG. 6: The cosmological parameters associated with the dark photon models in Fig. 5 with the same color coding as in Fig. 5. Shown are the dark photon lifetime and its abundance $\Omega_\gamma h^2$, in particular, the contribution the the present critical density dark photons would have if they did not decay. Note that h is the present Hubble constant in units of $100 \text{ km s}^{-1} \text{ Mpc}^{-1}$.

from extragalactic low-metallicity HII regions and an extrapolation to zero metallicity [90]. In our figures we also indicate regions where an important ${}^6\text{Li}$ production of ${}^6\text{Li}/{}^7\text{Li} > 0.1$ occurs. However, though the observational upper limit on ${}^6\text{Li}$ in the atmospheres of low-metallicity Pop II stars is approximately ${}^6\text{Li}/{}^7\text{Li} \lesssim 0.05$, such regions should strictly speaking not be considered ruled out, as ${}^6\text{Li}$ is very fragile and may have been destroyed in these stars from an initially higher level. This becomes particularly likely since ${}^7\text{Li}$ in the atmospheres of such stars is mostly observed in the range $1 \times 10^{-10} \lesssim {}^7\text{Li}/\text{H} \lesssim 2.5 \times 10^{-10}$ [91] as opposed to the expected primordial prediction of ${}^7\text{Li}/\text{H} \approx 5 \times 10^{-10}$ in standard BBN. The leading astrophysical explanation for this discrepancy is ${}^7\text{Li}$ destruction in low-metallicity Pop II stars due to an unknown mixing process in such stars. If this, indeed, is the case, ${}^6\text{Li}$ will be destroyed by even a larger factor than ${}^7\text{Li}$ as it is more fragile, and thus is not readily usable as constraint. However, an alternative explanation of the "cosmological lithium problem" is a destruction of ${}^7\text{Li}$ (often concomitant with production of ${}^6\text{Li}$) by the decay of relic particles [92]. This may also be achieved by decaying dark photons or dark Higgs with the right parameters. We thus show regions of parameter space

$$9 \times 10^{-11} < {}^7\text{Li}/\text{H} < 2.5 \times 10^{-10}, \quad (\text{V.5})$$

where the ${}^7\text{Li}$ problem is supposed to be strongly alleviated or solved by the decay of such particles. Finally, in a very small parameter space constraints apply from the potential underproduction of ${}^7\text{Li}$, we adopt ${}^7\text{Li}/\text{H} > 9 \times 10^{-11}$ as a conservative constraint.

A. BBN Constraints on Dark Photons

The lifetime of the dark photon is shown in Fig. 3. It is seen that for sufficiently small ϵ and $m_{\gamma'}$ it may be much longer than $\tau \sim 1$ sec. As the dark photon shares the quantum numbers of the photon, decay occurs into charged particles, whenever kinematically allowed. Note that decay into light quarks is kinematically blocked already for $m_{\gamma'} < 2m_{\pi^0}$ as otherwise hadronization may not occur. When $m_{\gamma'}$ approaches $2m_e$ from above the lifetime increases due to reduced phase space in the decay into e^\pm . For $m_{\gamma'} < 2m_e$ decay has to occur over a loop diagram into three photons with the respective lifetime becoming very long. This case is not treated in what follows.

In Fig. 5 the shaded colored regions show all the parameter space which is ruled out from a comparison between predicted and observationally inferred abundances. The constraints are from ${}^4\text{He}$ overproduction (green), ${}^2\text{H}$

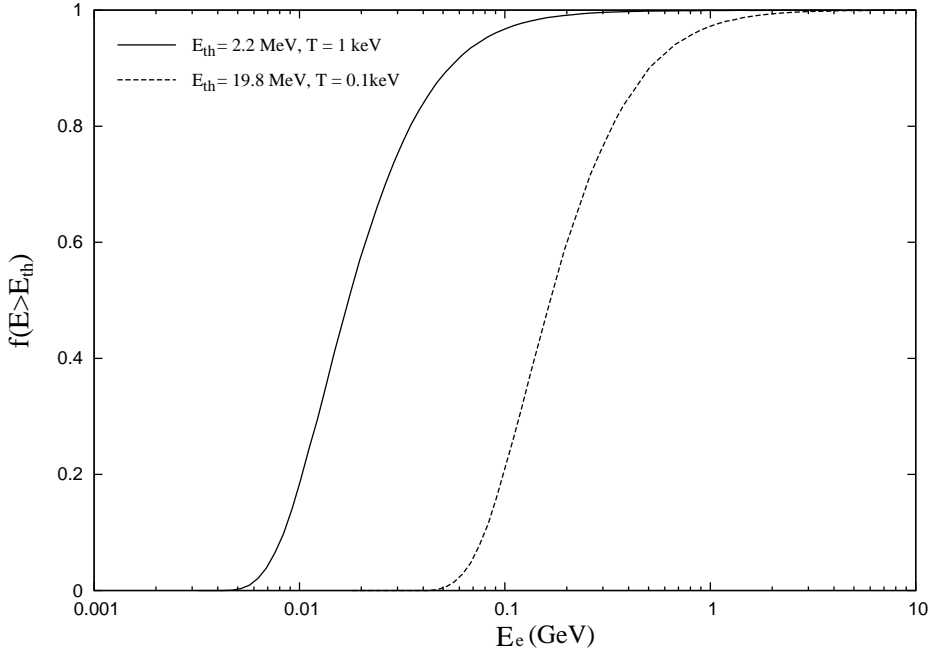


FIG. 7: The fraction of energy converted into photons capable of photodisintegration either ${}^2\text{H}$ or ${}^4\text{He}$, produced when electron-positron pairs of energy $2E_e$ are injected. Two examples are shown, (a) injection of pairs at cosmic temperature $T = 1\text{ keV}$ and $E_{th} = 2.2\text{ MeV}$ for deuterium photodisintegration, and (b) $T = 0.1\text{ keV}$ and $E_{th} = 19.8\text{ MeV}$ for helium photodisintegration. It is seen that in both cases the electron (positron) energy E_e has to be a factor ten larger in order to reach fractions of order one half.

overproduction (red), and ${}^2\text{H}$ underproduction (blue). The light grey area indicates parameter space where the cosmological ${}^7\text{Li}$ problem could be alleviated/solved, whereas the grey area indicates significant ${}^6\text{Li}$ production. Also shown in this figure by the solid line, is shown of how much the ${}^2\text{H}$ overproduction region would grow if a more aggressive limit of ${}^2\text{H}/\text{H} < 3 \times 10^{-5}$ would be imposed. These results thus confirm the known conclusion that solutions to the ${}^7\text{Li}$ problem through the decay of massive relic particle may not be attained without some additional ${}^2\text{H}/\text{H}$ production. In particular, no scenario solving the ${}^7\text{Li}$ problem with decaying dark photons achieves ${}^2\text{H}/\text{H} < 3 \times 10^{-5}$.

In Fig. 6, the predicted abundances $\Omega_{\gamma'} h^2$ and lifetimes $1/\Gamma_{\gamma'}$ for the models excluded in Fig. 5 are shown with the same color coding. It is noted that well-known trends are followed, i.e. relic particles hadronically decaying, (i.e. $m_{\gamma'} > 2m_{\pi}$ with shorter lifetimes $\tau \sim 1\text{ sec}$ but higher abundances $\Omega_{\gamma'} h^2$ are mostly constrained by ${}^4\text{He}$ overproduction, hadronically decaying relics with $\tau \sim 1000\text{ sec}$ and $\Omega h^2 \sim 10^{-3} - 10^{-4}$ are constrained by ${}^2\text{H}$ overproduction, and electromagnetically or hadronically decaying relics with longer lifetimes $\tau \gtrsim 10^5\text{ sec}$ may be constrained by ${}^2\text{H}$ underproduction. However, one usual trend is not observed in these figures. For the typical massive decaying particle stringent constraints apply at $\tau \gtrsim 3 \times 10^6\text{ sec}$ at already fairly low Ωh^2 due to ${}^4\text{He}$ photodisintegration and the concomitant ${}^3\text{He}/{}^2\text{H}$ overproduction. This has also been claimed by the recent analysis of Ref. [70] for the case of the dark photon. Usually injected energetic e^{\pm} rapidly inverse Compton scatter on the CMBR, with the resultant γ -rays pair-producing e^{\pm} pairs on the CMBR, leading to a new lower energy generation of e^{\pm} . The process repeats itself until the resulting γ -rays have energy $E_{\gamma} \lesssim E_{\gamma}^{e^{\pm}} \approx m_e^2/(20T)$ and are no longer sufficiently energetic to further pair-produce on thermal CMBR photons. When the cosmic temperature is low enough, such γ -rays may then photodisintegrate ${}^2\text{H}$ and ${}^4\text{He}$ with photodisintegration thresholds $E_{\gamma}^{th} = 2.2\text{ MeV}$ and 19.8 MeV , respectively. Such a scenario has been erroneously assumed by Ref. [70]. However, for the particular $\tau_{\gamma'} - m_{\gamma'}$ relation imposed by the dark photon interactions, the energy of injected e^{\pm} due to dark photon decay is often below $E_{\gamma}^{e^{\pm}}$. Moreover, for most of the parameter space the injected energies of e^{\pm} are so low that they are well in the Thomson scattering regime, i.e. $E_e \ll m_e^2/T$ (as opposed to the relativistic Klein-Nishina scattering regime). It is well known that inverse Compton scattering of e^{\pm} with energy E_e in the Thomson scattering regime leads to a multitude of softer photons with $E_{\gamma} \ll E_e$, rather than to a smaller number of energetic γ -rays with $E_{\gamma} \sim E_e$. This is exemplified by an accurate calculation shown in Fig. 7, which shows the fraction of produced γ -rays capable

of photodisintegrating ${}^2\text{H}$ and $T = 1\text{ keV}$ of ${}^4\text{He}$ at $T = 0.1\text{ keV}$ as a function of dark photon mass. It is seen that for $m_{\gamma'}$ too small, this fraction becomes very small, though naively one would expect photodisintegration to be possible as $m_{\gamma'} \gg E_{\gamma}^{th}$. The region enclosed by the dashed line in Fig. 5 and Fig. 6 thus shows parameter space which lead to a slightly elevated ${}^3\text{He}/{}^2\text{H}$ ratio, nevertheless, far from being ruled out.

B. BBN Constraints on Dark Higgses

Decay times of dark Higgs for fixed mixing angle span a much larger range than those of dark photons. This may be seen in Fig. 4. The dark Higgs has the same interactions with standard model particles as the Higgs particle up to an overall factor of ϵ . As such, its lifetime scales $1/(\epsilon^2 m^2)$, where m is the mass of the standard model particles arising from the dominant decay. Thus, whenever a channel becomes kinematically forbidden at $m_\rho < 2m_1$, decay predominantly occurs to the heaviest of all the lighter particles where decay is not kinematically forbidden. If this particle has mass m_2 , the decay time increases essentially instantaneously by $(m_1/m_2)^2$. This trend can be seen in Fig. 4, where sudden increases of τ_ρ are observed, as for example at $m_\rho \approx 2m_\pi$ where predominant decay switches first from hadrons to μ^\pm and then quickly to e^\pm yielding an about five order of magnitude increase in the decay time. The arguments above of course do not apply to loop-diagram decay into photons ($\gamma\gamma$) and gluons (gg). However, these decay channels are only important in very narrow intervals, as for example seen in the branching ratio in Fig. 4, which shows that decay $\rho \rightarrow \gamma\gamma$ dominates only when m_ρ comes too close to the $\rho \rightarrow ee^+$ threshold. For such low m_ρ dark Higgs decay may occur with lifetimes comparable or longer than the lifetime of the current Universe. Treating the important x - and γ -ray constraint which should apply in this regime is beyond the scope of the current paper, such that our CMBR analysis below only treats the regime $m_\rho > 2\text{ MeV}$.

In Fig. 8 BBN constraints on dark Higgses in the mass-mixing angle plane are shown. The color coding is as in Fig. 5, except for the purple regions which are ruled out by ${}^3\text{He}/{}^2\text{H}$ overproduction and the very small light-blue regions which are ruled out by ${}^7\text{Li}$ underproduction. Though similar arguments as for the dark photon, concerning the efficiency of ${}^4\text{He}$ photodisintegration in the Thomson scattering regime apply to the dark Higgs, since their decay channel below $m_\rho < 2m_\pi$ is also into electrons, large areas are ruled out from ${}^3\text{He}/{}^2\text{H}$ overproduction simply because the abundance of dark Higgses is typically larger than that of dark photons. This may be seen from Fig. 9 which shows the ruled out τ_ρ - Ω_ρ plane for the same models as in Fig. 8. Some of the possible τ_ρ - Ω_ρ parameter space is not covered, as the constraints come on separated lines in the τ_ρ - Ω_ρ plane. This is simply an artifact due to our grid spacing of 1.06 in m_ρ (as well as in ϵ). For jumps in τ_ρ as large as 10^5 over a narrow m_ρ interval not all possible decay times are resolved, leading to this line structure, with individual neighboring lines separated by in mass by a factor 1.06.

We note that the ${}^7\text{Li}$ problem can be solved at $\epsilon \sim 10^{-7}$ and $m_\rho \approx 3.5\text{ MeV}$. This portion of parameter space is close to regions which are ruled out by ${}^7\text{Li}$ underproduction, i.e. ${}^7\text{Li} < 9 \times 10^{-11}$. We call attention to this particular region, even though it is small, as it is the only currently known solution to the ${}^7\text{Li}$ problem by decay of relic particles which does (*not*) lead to additional ${}^2\text{H}$ production or destruction. The reason for this is simple; the injection of e^\pm with energy 1.75 GeV may lead to γ -rays of energy which are capable of photodisintegrating ${}^7\text{Be}$ with photodisintegration threshold of 1.58 MeV but not ${}^2\text{H}$ with threshold 2.2 MeV . As at earlier times most of the primordial ${}^7\text{Li}$ is still in form of ${}^7\text{Be}$ before electron-capturing to form ${}^7\text{Li}$ after 53 days, this becomes possible. Most other ${}^7\text{Li}$ solving scenarios rely on injection of neutrons which lead to an additional ${}^2\text{H}$ production via neutron capture on protons.

However, it is currently not clear if these already small ${}^7\text{Li}$ solving regions do not become even smaller by ${}^4\text{He}$ overproduction. We have noted that the typical abundances of dark Higgs are large. In fact they are so large that they may come close to their thermal equilibrium abundance in some part of parameter space at very large ϵ . It is well known that substantial extra energy density over that of the standard model plasma, present at the onset of BBN at $\tau \sim 1\text{ sec}$, leads to an increase of the ${}^4\text{He}$ abundance due to an increase in the cosmic expansion rate. Such limits are often stated in terms of extra putative neutrino (light) degrees of freedom present in the plasma, with ΔN_ν constrained to be smaller than $\sim 1 - 2$. Note that the energy density ΔN_ν at $T \sim 1\text{ MeV}$ corresponds very approximately to $\Omega_\rho h^2 \sim 3 \times 10^4$ in dark Higgs abundance. Such large values of $\Omega_\rho h^2$ with lifetimes $\tau \gtrsim 1\text{ sec}$ are reached in the low-mass, high mixing angle region, approximately for $\epsilon \gtrsim 10^{-6} - 10^{-7}$ and $2\text{ MeV} \lesssim m_\rho \lesssim 300\text{ MeV}$. Of course, dark Higgs of $m_\rho > 1\text{ MeV}$ are not exactly light degrees of freedom at $T \lesssim 1\text{ MeV}$. Their energy density redshifts differently than that of light degrees of freedom. At such large interaction strength it may also be possible that dark Higgs will again be destroyed before BBN by process such as $\gamma\rho \rightarrow e^-e^+$. All these effects are not included in the current analysis as they are beyond the scope of the paper. In particular, BBN codes with decaying or annihilating particles do usually not include such effects, as constraints are already usually stringent for much smaller abundances. We only note here, that the very upper left-hand corner of Fig. 8 is tagged to be potentially ruled out by ${}^4\text{He}$ overproduction and leave exact results for future work.

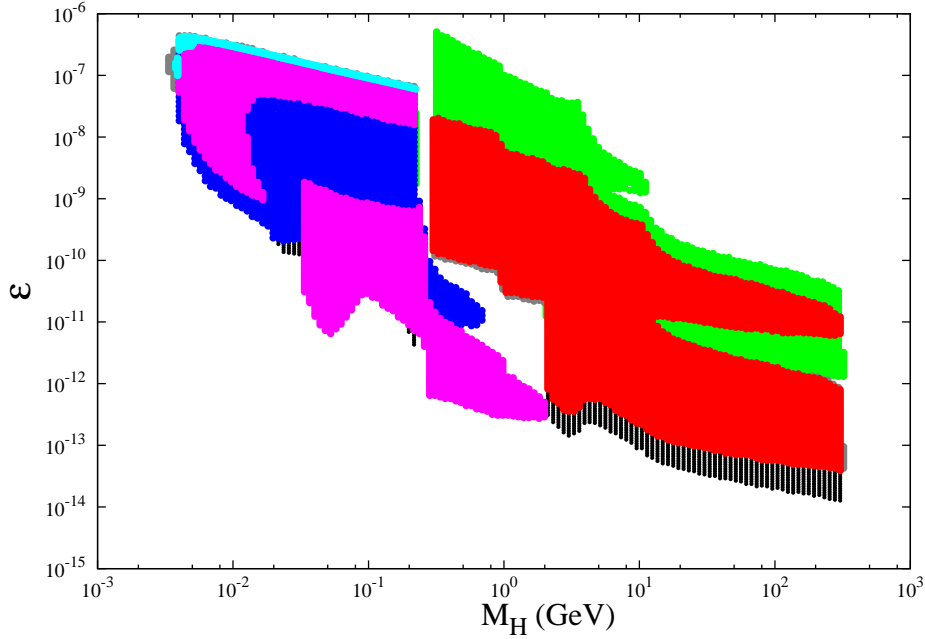


FIG. 8: The constraints on the dark Higgs parameter space with the color/line coding as in Fig. 6. Solid purple areas are ruled out due to an overproduction of the ${}^3\text{He}/{}^2\text{D}$ ratio, i.e. ${}^3\text{He}/{}^2\text{D} > 1.5$.

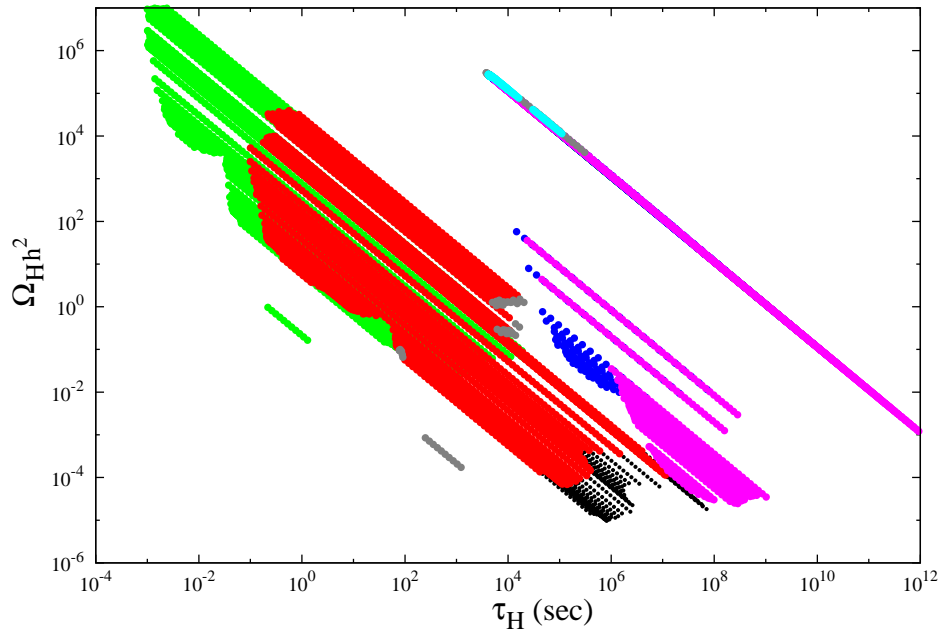


FIG. 9: The Higgs abundances and lifetimes associated with the dark Higgs parameter space ruled out as shown in Fig. 8.

VI. COSMIC MICROWAVE BACKGROUND CONSTRAINTS

Precise observations of the CMBR have proven to be an invaluable tool for determining cosmological parameters, as well as constraining models of the early Universe beyond the standard model. Observations of anisotropies in the CMBR, as well as limits on deviations from a perfect blackbody spectrum of the CMBR, have to be confronted by theoretical predictions for any particular model. The Planck and WMAP satellite missions, as well as a large

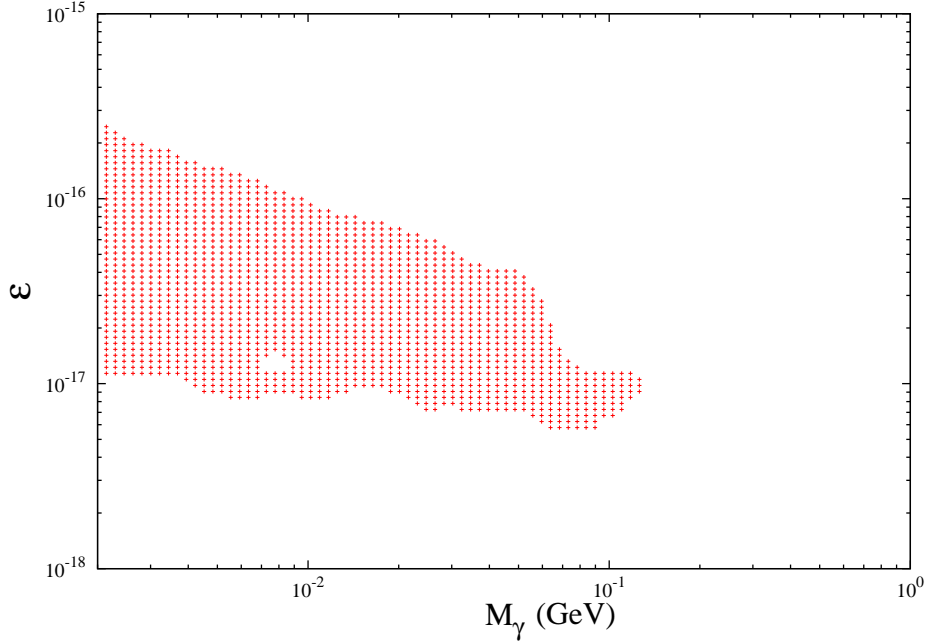


FIG. 10: The shaded region indicates dark photon models which are ruled out by current observations of anisotropies in the CMBR.

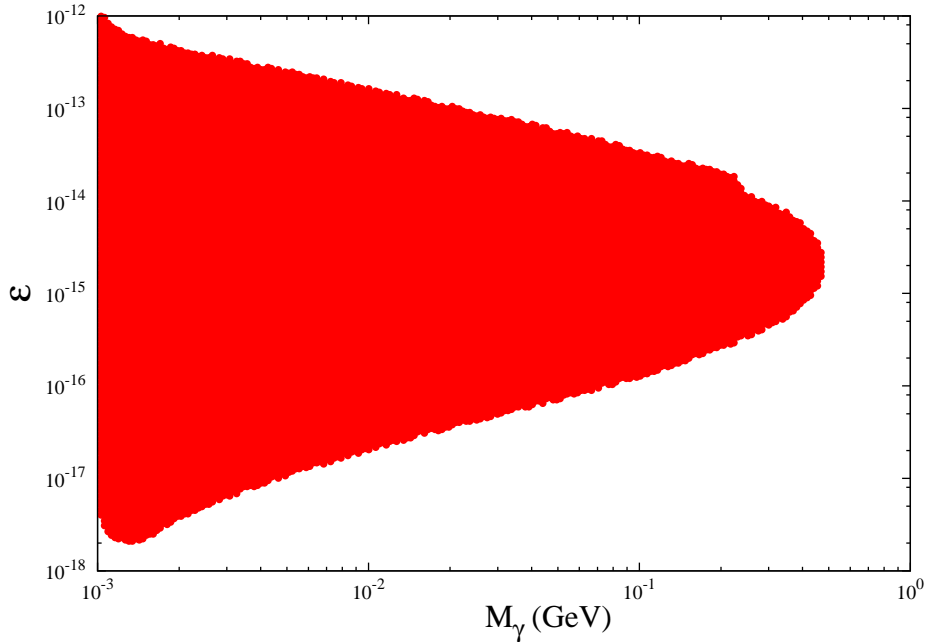


FIG. 11: Dark photon model which could be ruled out by a future PIXIE mission.

number of ballone-type experiments, have observed anisotropies in the CMBR, whereas the FIRAS-instrument on the COBE satellite has limited deviations from an ideal Planck spectrum, to be approximately below one part in 10^4 [93]. The latter limits may be potentially improved by 3 to 4 orders of magnitude by a dedicated satellite mission named PIXIE [94].

The effects of annihilation and decay of relic particles on the anisotropies of the CMBR have already been analyzed in a number of prior publications. See for example [95] and the references therein. Injecting energetic photons and/or electrons into the plasma starts a cascade on the CMBR, producing a multitude of secondary lower

energy electrons and photons. When their energy falls below $E \sim 10$ keV their main effect is the ionization and accompanying heating of neutral hydrogen and helium. If the decay happens shortly before, during, or somewhat after recombination, an additional (scale-dependent) suppression of the primary anisotropies by additional scattering of CMBR photons on free electrons results. Though this effect may be partially compensated for by increasing the normalization A_s and the spectral index n_s of the scalar primordial perturbations, the precise observations of the high- l TT anisotropy spectrum still results in important constraints.

In this study we have modified the recombination routine RECFAST [96] to include energy injection, employing the detailed cascade results of Ref. [97]. We assume that 1/3 of the energy of $E \lesssim 10$ keV e^- 's and γ 's goes into ionization, whereas 2/3 into heating. The modified recombination routine was then used with the CMBR code CAMB and the Markov-Chain Monte-Carlo (i.e. MCMC) code COSMOMC [98] to derive constraints on dark photons and dark Higgses decaying around recombination. In our MCMC analysis we take very generous priors on cosmological parameters, in particular generous on n_s and A_s , to avoid missing degenerate good fits to the data. Results are produced typically by calculating of the order 2×10^6 to 5×10^6 models, and calculating their likelihood that they may produce the observed data.

It is well known that the injection of energetic e^\pm 's and γ 's before recombination (as well as after in the case of e^\pm) leads to spectral distortions in the CMBR energy spectrum, since the energy injected may not be anymore entirely thermalized when injected below redshift $z \lesssim 3 \times 10^6$ (temperature $T \lesssim 1$ keV). This leads to non-vanishing chemical potential μ deviations for $z \lesssim 3 \times 10^6$, since photon number changing double Compton-scattering is no longer efficient at these lower redshifts to produce the correct number of photons in the spectrum, and spectral y distortions for $z \lesssim 4 \times 10^4$ as even Thomson scattering may then no longer completely equilibrate the distribution. Such limits are generic, and may be stated as an upper limit on the fractional energy $\Delta\epsilon^{\text{inj}}/\epsilon^{\text{CMBR}}$ of the total CMBR energy density, which is due to non-thermal injection. The FIRAS instrument imposes $\Delta\epsilon^{\text{inj}}/\epsilon^{\text{CMBR}} \lesssim 6 \times 10^{-5}$. A future PIXIE mission would hope to reach the sensitivity of $\Delta\epsilon^{\text{inj}}/\epsilon^{\text{CMBR}} \lesssim 10^{-8}$. However, it should be noted that at such low $\Delta\epsilon^{\text{inj}}/\epsilon^{\text{CMBR}} \sim 10^{-8}$ other standard sources such as Silk-damping could become foregrounds. In any case, such considerations set important limits already now, particularly for the typical large predicted abundances of dark Higgs.

A. CMB Constraints on Dark Photons

Fig. 10 shows by the shaded area dark photon models in the mass - mixing angle plane which are ruled out by the precise observations of the angular anisotropies of the CMBR. Here we used recent Planck data [99] for our analysis. In general about as much parameter space is ruled by the CMBR as by BBN, however, at lower masses and smaller mixing angles, leading to decay around recombination. A small island of allowed models surrounded by disallowed models is noted in this figure. This is due to a statistical fluctuation, since the entire ruled out region is not ruled out by a large likelihood degradation. There are no constraints on dark photon parameters from current FIRAS limits on deviations from a blackbody spectrum. In Fig. 11 possible limits are shown after a successful PIXIE mission [94]. Here a maximal sensitivity of $\Delta\epsilon^{\text{inj}}/\epsilon^{\text{CMBR}} \sim 10^{-8}$ has been assumed. It is seen that such limits could rule out a multiple of the parameter space currently ruled out by the anisotropies of the CMBR, of course, assuming that known foregrounds could be controlled.

B. CMB Constraints on Dark Higgs

Limits on dark Higgs parameters from the anisotropies of the CMBR are shown in Fig. 12. Here as well somewhat disconnected pieces may be observed, one at lower mass where the decay channel is $\rho \rightarrow e^-e^+$, and one at somewhat higher masses where the main decay channel is $\rho \rightarrow$ hadrons, and where the ρ lifetime is considerably smaller for the same ϵ . In contrast to the case of the dark photon, due to the high ρ abundances, the ruled out regions show a very significant degrade in the likelihood, i.e. are strongly ruled out. In Fig. 13 limits on the dark Higgs are shown from possible μ and y -type deviations of the Planck spectrum. Here the large green area is ruled out by the current FIRAS limit, whereas it would only somewhat extend to the red area with a successful PIXIE mission.

VII. CONCLUSIONS

Bosonic mediators generically arise in models with a hidden dark sector. In terms of models with renormalizable interactions, the only two bosonic possibilities are a dark photon that kinetically mixes with the standard model photon/ Z and a dark Higgs that mixes with the standard model Higgs. Light mediators with masses $m \lesssim 100$ GeV

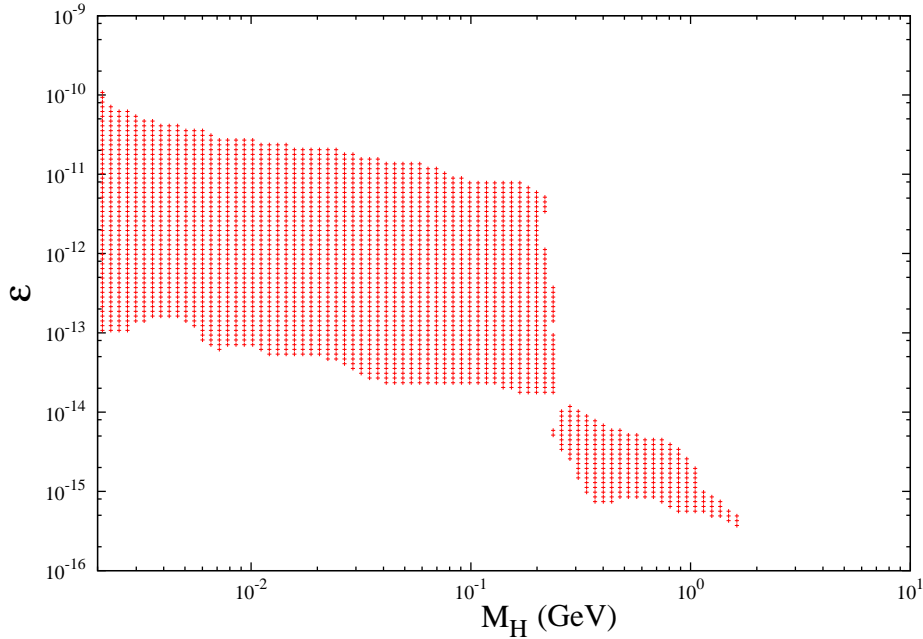


FIG. 12: Dark Higgs model ruled out by Planck data.

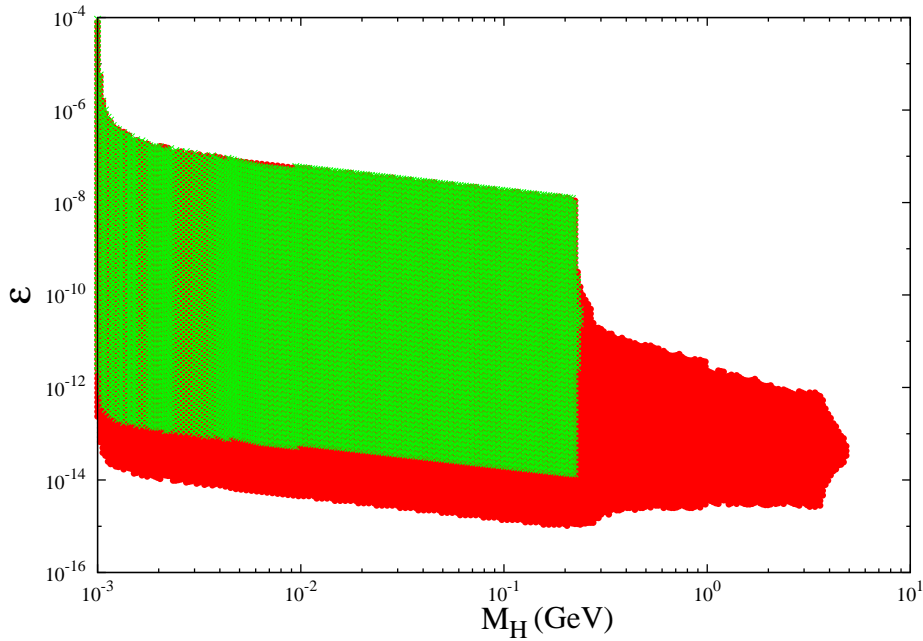


FIG. 13: Dark Higgs model currently ruled out by deviations of the CMBR from a blackbody spectrum (green). The red area shows how much these limits would extend after a PIXIE mission.

are kinematically accessible in experiments, yet can evade detection in accelerator and beam dump experiments if they have extremely weak interactions with the standard model. When the mixing becomes extremely weak the existence of such particles can be tested by cosmology. In this work, we have performed a detailed study of these tests. Assuming conservatively that their abundance is negligible at the end of inflation they will nevertheless be produced in small abundance by two-body interactions in the thermal standard model plasma, with their non-equilibrium abundance governed by the small mixing parameter ϵ , a process dubbed freeze-in. Due to the smallness of ϵ they become long-lived particles subsequently decaying back into the visible sector. If this decay occurs after

the onset of BBN, stringent constraints may be derived from the distortion of the light-element nucleosynthesis, the distortion of the CMB blackbody spectrum, as well as the alteration of the angular anisotropies in the CMB.

We have found that large parts of parameter space at very small mixing $\epsilon \sim 10^{-6} - 10^{-14}$ are already constrained, or can be constrained by future missions such as PIXIE. Our results begin the important task of constraining the small mixing angle regions of models in which a mediator mixes with a standard model boson. We further find that in very small parts of parameter space such exotic particles could solve the cosmological lithium problem.

Several directions for further study are possible within the context of these models. For very light mediators, below around 1 MeV, new decay modes and signals open up. For dark Higgs, the dominant decay is to a pair of photons. For dark photons, decays to two photons are forbidden by the Landau-Yang theorem. Nevertheless, loop-induced decays to three photons are possible. Either case could yield interesting signals in the cosmological x-ray and gamma-ray backgrounds. For large mixing angles, the mediator may thermalize with the standard model before decaying. Such a scenario has been mentioned in the text above, but it would be interesting to verify the cosmological constraints in detail. The addition of a stable dark matter particle to the scenario discussed in this work could lead to a viable model of either thermal or non-thermal cold dark matter production. The simple models we have examined potentially have a very rich phenomenology that remains to be explored further.

Acknowledgments: We thank D. Finkbeiner for collaborating during the early stages of this project. We also thank R. Caldwell, D. Curtin, S. El Hedri, R. Mohapatra, S. Nussinov, and T. Slatyer for useful conversations. JB is supported by the U. S. Department of Energy under the contract DE-FG-02-95ER40896. DW is supported by a grant from the University of Washington. Part of this work was completed at SLAC, which is operated by Stanford University for the US Department of Energy under contract DE-AC02-76SF00515.

-
- [1] B. Holdom, Phys. Lett. B **166**, 196 (1986). doi:10.1016/0370-2693(86)91377-8
 - [2] F. Del Aguila, Acta Phys. Polon. B **25**, 1317 (1994) [hep-ph/9404323].
 - [3] F. Del Aguila, M. Cvetič and P. Langacker, Phys. Rev. D **52**, 37 (1995) doi:10.1103/PhysRevD.52.37 [hep-ph/9501390].
 - [4] K. S. Babu, C. F. Kolda and J. March-Russell, Phys. Rev. D **54**, 4635 (1996) doi:10.1103/PhysRevD.54.4635 [hep-ph/9603212].
 - [5] K. S. Babu, C. F. Kolda and J. March-Russell, Phys. Rev. D **57**, 6788 (1998) [hep-ph/9710441].
 - [6] R. Foot, H. Lew and R. R. Volkas, Mod. Phys. Lett. A **7**, 2567 (1992). doi:10.1142/S0217732392004031
 - [7] Z. Chacko, H. S. Goh and R. Harnik, Phys. Rev. Lett. **96**, 231802 (2006) doi:10.1103/PhysRevLett.96.231802 [hep-ph/0506256].
 - [8] R. Barbieri, T. Gregoire and L. J. Hall, hep-ph/0509242.
 - [9] W. F. Chang, J. N. Ng and J. M. S. Wu, Phys. Rev. D **74**, 095005 (2006) [Phys. Rev. D **79**, 039902 (2009)] doi:10.1103/PhysRevD.74.095005, 10.1103/PhysRevD.79.039902 [hep-ph/0608068].
 - [10] V. Barger, P. Langacker, M. McCaskey, M. J. Ramsey-Musolf and G. Shaughnessy, Phys. Rev. D **77**, 035005 (2008) doi:10.1103/PhysRevD.77.035005 [arXiv:0706.4311 [hep-ph]].
 - [11] M. J. Strassler and K. M. Zurek, Phys. Lett. B **661**, 263 (2008) doi:10.1016/j.physletb.2008.02.008 [hep-ph/0605193].
 - [12] M. J. Strassler and K. M. Zurek, Phys. Lett. B **651**, 374 (2007) doi:10.1016/j.physletb.2007.06.055 [hep-ph/0604261].
 - [13] O. Lebedev and H. M. Lee, Eur. Phys. J. C **71**, 1821 (2011) doi:10.1140/epjc/s10052-011-1821-0 [arXiv:1105.2284 [hep-ph]].
 - [14] W. F. Chang, J. N. Ng and J. M. S. Wu, Phys. Rev. D **75**, 115016 (2007) doi:10.1103/PhysRevD.75.115016 [hep-ph/0701254 [HEP-PH]].
 - [15] C. Englert, T. Plehn, D. Zerwas and P. M. Zerwas, Phys. Lett. B **703**, 298 (2011) doi:10.1016/j.physletb.2011.08.002 [arXiv:1106.3097 [hep-ph]].
 - [16] V. Silveira and A. Zee, Phys. Lett. B **161**, 136 (1985). doi:10.1016/0370-2693(85)90624-0
 - [17] J. D. Wells, In *Kane, Gordon (ed.), Pierce, Aaron (ed.): Perspectives on LHC physics* 283-298 [arXiv:0803.1243 [hep-ph]].
 - [18] R. Schabinger and J. D. Wells, Phys. Rev. D **72**, 093007 (2005) doi:10.1103/PhysRevD.72.093007 [hep-ph/0509209].
 - [19] M. Bowen, Y. Cui and J. D. Wells, JHEP **0703**, 036 (2007) doi:10.1088/1126-6708/2007/03/036 [hep-ph/0701035].
 - [20] R. Foot, H. Lew and R. R. Volkas, Phys. Lett. B **272**, 67 (1991). doi:10.1016/0370-2693(91)91013-L
 - [21] B. Patt and F. Wilczek, hep-ph/0605188.
 - [22] C. Englert, J. Jaeckel, V. V. Khoze and M. Spannowsky, JHEP **1304**, 060 (2013) doi:10.1007/JHEP04(2013)060 [arXiv:1301.4224 [hep-ph]].
 - [23] K. Kumar, R. Vega-Morales and F. Yu, Phys. Rev. D **86**, 113002 (2012) [Phys. Rev. D **87**, no. 11, 119903 (2013)] doi:10.1103/PhysRevD.87.119903, 10.1103/PhysRevD.86.113002 [arXiv:1205.4244 [hep-ph]].
 - [24] C. Englert, arXiv:1204.4579 [hep-ph].
 - [25] L. Lopez-Honorez, T. Schwetz and J. Zupan, Phys. Lett. B **716**, 179 (2012) doi:10.1016/j.physletb.2012.07.017 [arXiv:1203.2064 [hep-ph]].
 - [26] O. Lebedev, Eur. Phys. J. C **72**, 2058 (2012) doi:10.1140/epjc/s10052-012-2058-2 [arXiv:1203.0156 [hep-ph]].

- [27] B. Batell, S. Gori and L. T. Wang, JHEP **1206**, 172 (2012) doi:10.1007/JHEP06(2012)172 [arXiv:1112.5180 [hep-ph]].
- [28] A. Djouadi, O. Lebedev, Y. Mambrini and J. Quevillon, Phys. Lett. B **709**, 65 (2012) doi:10.1016/j.physletb.2012.01.062 [arXiv:1112.3299 [hep-ph]].
- [29] C. Englert, T. Plehn, M. Rauch, D. Zerwas and P. M. Zerwas, Phys. Lett. B **707**, 512 (2012) doi:10.1016/j.physletb.2011.12.067 [arXiv:1112.3007 [hep-ph]].
- [30] S. Baek, P. Ko and W. I. Park, JHEP **1202**, 047 (2012) doi:10.1007/JHEP02(2012)047 [arXiv:1112.1847 [hep-ph]].
- [31] O. Lebedev, H. M. Lee and Y. Mambrini, Phys. Lett. B **707**, 570 (2012) doi:10.1016/j.physletb.2012.01.029 [arXiv:1111.4482 [hep-ph]].
- [32] I. Brivio, M. B. Gavela, L. Merlo, K. Mimasu, J. M. No, R. del Rey and V. Sanz, arXiv:1511.01099 [hep-ph].
- [33] S. Sun, arXiv:1510.02309 [hep-ph].
- [34] A. Freitas, S. Westhoff and J. Zupan, JHEP **1509**, 015 (2015) doi:10.1007/JHEP09(2015)015 [arXiv:1506.04149 [hep-ph]].
- [35] M. A. Fedderke, T. Lin and L. T. Wang, arXiv:1506.05465 [hep-ph].
- [36] V. V. Khoze, G. Ro and M. Spannowsky, Phys. Rev. D **92**, no. 7, 075006 (2015) doi:10.1103/PhysRevD.92.075006 [arXiv:1505.03019 [hep-ph]].
- [37] F. Bishara, J. Brod, P. Uttayarat and J. Zupan, arXiv:1504.04022 [hep-ph].
- [38] W. Chao and M. J. Ramsey-Musolf, arXiv:1503.00028 [hep-ph].
- [39] A. Falkowski, C. Gross and O. Lebedev, JHEP **1505**, 057 (2015) doi:10.1007/JHEP05(2015)057 [arXiv:1502.01361 [hep-ph]].
- [40] W. Chao, Phys. Rev. D **92**, no. 1, 015025 (2015) doi:10.1103/PhysRevD.92.015025 [arXiv:1412.3823 [hep-ph]].
- [41] Z. Chacko, Y. Cui and S. Hong, Phys. Lett. B **732**, 75 (2014) doi:10.1016/j.physletb.2014.03.010 [arXiv:1311.3306 [hep-ph]].
- [42] S. Y. Choi, C. Englert and P. M. Zerwas, Eur. Phys. J. C **73**, 2643 (2013) doi:10.1140/epjc/s10052-013-2643-z [arXiv:1308.5784 [hep-ph]].
- [43] J. P. Lees *et al.* [BaBar Collaboration], Phys. Rev. Lett. **113**, no. 20, 201801 (2014) doi:10.1103/PhysRevLett.113.201801 [arXiv:1406.2980 [hep-ex]].
- [44] J. Blumlein and J. Brunner, Phys. Lett. B **701**, 155 (2011) doi:10.1016/j.physletb.2011.05.046 [arXiv:1104.2747 [hep-ex]].
- [45] S. Andreas, C. Niebuhr and A. Ringwald, Phys. Rev. D **86**, 095019 (2012) doi:10.1103/PhysRevD.86.095019 [arXiv:1209.6083 [hep-ph]].
- [46] M. Endo, K. Hamaguchi and G. Mishima, Phys. Rev. D **86**, 095029 (2012) doi:10.1103/PhysRevD.86.095029 [arXiv:1209.2558 [hep-ph]].
- [47] D. Babusci *et al.* [KLOE-2 Collaboration], Phys. Lett. B **720**, 111 (2013) doi:10.1016/j.physletb.2013.01.067 [arXiv:1210.3927 [hep-ex]].
- [48] D. Babusci *et al.* [KLOE-2 Collaboration], Phys. Lett. B **736**, 459 (2014) doi:10.1016/j.physletb.2014.08.005 [arXiv:1404.7772 [hep-ex]].
- [49] P. Adlarson *et al.* [WASA-at-COSY Collaboration], Phys. Lett. B **726**, 187 (2013) doi:10.1016/j.physletb.2013.08.055 [arXiv:1304.0671 [hep-ex]].
- [50] G. Agakishiev *et al.* [HADES Collaboration], Phys. Lett. B **731**, 265 (2014) doi:10.1016/j.physletb.2014.02.035 [arXiv:1311.0216 [hep-ex]].
- [51] J. Blmlein and J. Brunner, Phys. Lett. B **731**, 320 (2014) doi:10.1016/j.physletb.2014.02.029 [arXiv:1311.3870 [hep-ph]].
- [52] H. Merkel *et al.*, Phys. Rev. Lett. **112**, no. 22, 221802 (2014) doi:10.1103/PhysRevLett.112.221802 [arXiv:1404.5502 [hep-ex]].
- [53] S. Abrahamyan *et al.* [APEX Collaboration], Phys. Rev. Lett. **107**, 191804 (2011) doi:10.1103/PhysRevLett.107.191804 [arXiv:1108.2750 [hep-ex]].
- [54] J. P. Lees *et al.* [BaBar Collaboration], Phys. Rev. Lett. **108**, 211801 (2012) doi:10.1103/PhysRevLett.108.211801 [arXiv:1202.1313 [hep-ex]].
- [55] B. Aubert *et al.* [BaBar Collaboration], arXiv:0908.2821 [hep-ex].
- [56] B. Aubert *et al.* [BaBar Collaboration], Phys. Rev. Lett. **103**, 081803 (2009) doi:10.1103/PhysRevLett.103.081803 [arXiv:0905.4539 [hep-ex]].
- [57] D. Kazanas, R. N. Mohapatra, S. Nussinov, V. L. Teplitz and Y. Zhang, Nucl. Phys. B **890**, 17 (2014) doi:10.1016/j.nuclphysb.2014.11.009 [arXiv:1410.0221 [hep-ph]].
- [58] B. Batell, R. Essig and Z. Surujon, Phys. Rev. Lett. **113**, no. 17, 171802 (2014) doi:10.1103/PhysRevLett.113.171802 [arXiv:1406.2698 [hep-ph]].
- [59] A. Anastasi *et al.*, Phys. Lett. B **750**, 633 (2015) doi:10.1016/j.physletb.2015.10.003 [arXiv:1509.00740 [hep-ex]].
- [60] R. Holzmann *et al.* [HADES Collaboration], doi:10.3204/DESY-PROC-2014-04/9
- [61] V. Khachatryan *et al.* [CMS Collaboration], Phys. Lett. B **752**, 146 (2016) doi:10.1016/j.physletb.2015.10.067 [arXiv:1506.00424 [hep-ex]].
- [62] G. Aad *et al.* [ATLAS Collaboration], arXiv:1511.05542 [hep-ex].
- [63] J. R. Batley *et al.* [NA48/2 Collaboration], Phys. Lett. B **746**, 178 (2015) doi:10.1016/j.physletb.2015.04.068 [arXiv:1504.00607 [hep-ex]].
- [64] A. Anastasi *et al.* [KLOE-2 Collaboration], Phys. Lett. B **747**, 365 (2015) doi:10.1016/j.physletb.2015.06.015 [arXiv:1501.06795 [hep-ex]].
- [65] I. Jaegle [Belle Collaboration], Phys. Rev. Lett. **114**, no. 21, 211801 (2015) doi:10.1103/PhysRevLett.114.211801 [arXiv:1502.00084 [hep-ex]].

- [66] A. Palladino, *Acta Phys. Polon. B* **46**, 65 (2015) doi:10.5506/APhysPolB.46.65 [arXiv:1501.05173 [hep-ex]].
- [67] F. Curciarello, *Acta Phys. Polon. B* **46**, 39 (2015) doi:10.5506/APhysPolB.46.39 [arXiv:1501.04424 [hep-ex]].
- [68] A. Adare *et al.* [PHENIX Collaboration], *Phys. Rev. C* **91**, no. 3, 031901 (2015) doi:10.1103/PhysRevC.91.031901 [arXiv:1409.0851 [nucl-ex]].
- [69] G. Aad *et al.* [ATLAS Collaboration], *JHEP* **1411**, 088 (2014) doi:10.1007/JHEP11(2014)088 [arXiv:1409.0746 [hep-ex]].
- [70] A. Fradette, M. Pospelov, J. Pradler and A. Ritz, *Phys. Rev. D* **90**, no. 3, 035022 (2014) [arXiv:1407.0993 [hep-ph]].
- [71] G. Aad *et al.* [ATLAS and CMS Collaborations], *Phys. Rev. Lett.* **114**, 191803 (2015) [arXiv:1503.07589 [hep-ex]].
- [72] G. Aad *et al.* [ATLAS Collaboration], arXiv:1507.04548 [hep-ex].
- [73] V. Khachatryan *et al.* [CMS Collaboration], *Eur. Phys. J. C* **75**, no. 5, 212 (2015) [arXiv:1412.8662 [hep-ex]].
- [74] L. J. Hall, K. Jedamzik, J. March-Russell and S. M. West, *JHEP* **1003**, 080 (2010) [arXiv:0911.1120 [hep-ph]].
- [75] T. Sjostrand, S. Mrenna and P. Z. Skands, *JHEP* **0605**, 026 (2006) doi:10.1088/1126-6708/2006/05/026 [hep-ph/0603175].
- [76] V. V. Ezhela, S. B. Lugovsky and O. V. Zenin, hep-ph/0312114.
- [77] K. A. Olive *et al.* [Particle Data Group Collaboration], *Chin. Phys. C* **38**, 090001 (2014).
- [78] E. Braaten and J. P. Leveille, *Phys. Rev. D* **22**, 715 (1980). doi:10.1103/PhysRevD.22.715
- [79] T. Inami, T. Kubota and Y. Okada, *Z. Phys. C* **18**, 69 (1983). doi:10.1007/BF01571710
- [80] J. F. Gunion, H. E. Haber, G. L. Kane and S. Dawson, *Front. Phys.* **80**, 1 (2000).
- [81] A. I. Vainshtein, V. I. Zakharov and M. A. Shifman, *Sov. Phys. Usp.* **23**, 429 (1980) [*Usp. Fiz. Nauk* **131**, 537 (1980)].
- [82] M. B. Voloshin, *Sov. J. Nucl. Phys.* **44**, 478 (1986) [*Yad. Fiz.* **44**, 738 (1986)].
- [83] K. Jedamzik, *Phys. Rev. D* **74**, 103509 (2006)
- [84] S. Burles and D. Tytler, *Astrophys. J.* **499**, 699 (1998)
- [85] S. Burles and D. Tytler, *Astrophys. J.* **507**, 732 (1998)
- [86] R. Cooke, M. Pettini, R. A. Jorgenson, M. T. Murphy and C. C. Steidel, *Astrophys. J.* **781**, no. 1, 31 (2014)
- [87] J. L. Linsky *et al.*, *Astrophys. J.* **647**, 1106 (2006) doi:10.1086/505556 [astro-ph/0608308].
- [88] G. Sigl, K. Jedamzik, D. N. Schramm and V. S. Berezinsky, *Phys. Rev. D* **52**, 6682 (1995)
- [89] G. Gloeckler and J. Geiss, *Light Elements and their evolution, IAU Symposia* **198**, 224 (2000).
- [90] Y. I. Izotov, G. Stasinska and N. G. Guseva, *Astron. Astrophys.* **558**, A57 (2013)
- [91] S. G. Ryan, T. C. Beers, K. A. Olive, B. D. Fields and J. E. Norris, *Astrophys. J.* **530**, L57 (2000); P. Bonifacio *et al.*, *Astron. Astrophys.* **462**, 851 (2007) A. Hosford, S. G. Ryan, A. E. G. Perez, J. E. Norris and K. A. Olive, *Astron. Astrophys.* **493**, 601 (2009); W. Aoki, P. S. Barklem, T. C. Beers, N. Christlieb, S. Inoue, A. E. G. Perez, J. E. Norris and D. Carollo, *Astrophys. J.* **698**, 1803 (2009); L. Sbordone *et al.*, *Astron. Astrophys.* **522**, A26 (2010).
- [92] K. Jedamzik, *Phys. Rev. D* **70**, 063524 (2004).
- [93] D. J. Fixsen, E. S. Cheng, J. M. Gales, J. C. Mather, R. A. Shafer and E. L. Wright, *Astrophys. J.* **473**, 576 (1996).
- [94] A. Kogut *et al.*, *JCAP* **1107**, 025 (2011).
- [95] D. P. Finkbeiner, S. Galli, T. Lin and T. R. Slatyer, *Phys. Rev. D* **85**, 043522 (2012) doi:10.1103/PhysRevD.85.043522.
- [96] S. Seager, D. D. Sasselov and D. Scott, *Astrophys. J.* **523**, L1 (1999).
- [97] T. R. Slatyer, *Phys. Rev. D* **87**, no. 12, 123513 (2013).
- [98] A. Lewis and S. Bridle, *Phys. Rev. D* **66**, 103511 (2002).
- [99] R. Adam *et al.* [Planck Collaboration], arXiv:1502.01582 [astro-ph.CO]; P. A. R. Ade *et al.* [Planck Collaboration], arXiv:1502.01589 [astro-ph.CO].